INTERNATIONAL JOURNAL OF
NUMERICAL ANALYSIS AND MODELING
Volume 5, Number 1, Pages 152–165

NUMERICAL CHARACTERIZATION OF THE REGULARITY LOSS IN MINIMAL SURFACES

MAKRAM HAMOUDA AND HERVÉ V.J. LE MEUR

(Communicated by R. Temam)

Abstract. In this article, we numerically study the regularity loss of the solutions of non-parametric minimal surfaces with non-zero boundary conditions. Parts of the boundaries have non-positive mean curvature. As expected from theoretical results in such geometry, we find that the solutions may or may not satisfy the boundary conditions depending upon the data. Firstly, we validate the numerical study on the astroid and discuss the various kinds of non-regularity characterizations. We provide an algorithm to test the regularity loss using the numerical results. Secondly, we give a numerical estimate of the threshold value of the boundary condition beyond which no regular solution exists. More theoretical results are also given on the approximation by the regularized solution of the non-regularized one. The regularized solution exhibits a boundary layer. Finally, the study is applied to the catenoid for which the exact threshold value is known. The exact value and the computed one are in good agreement.

Key Words. Boundary layers, minimal surfaces, non-regular solutions, singular perturbations.

1. Introduction

1.1. The context. Minimal surfaces have received attention at least since the publication of L. Euler's book [6] in 1744. In this book, L. Euler discussed one hundred problems, one of them being to find surfaces of revolution having a critical area. Later, J.L. Lagrange made the connection between vanishing mean curvature and the first variation of area [13]. From experiments, J.A.F. Plateau noticed that the singular set Γ of a soap bubble cluster is a piecewise smooth curve with vertices, satisfying two laws [14]. These laws were proved only in 1976 with the theory of varifolds by F. Almgren [1] and the regularity theorem of J. Taylor [19].

Almost two centuries and a half later, this topic is still active. In the Summer of 2001, the Mathematical Sciences Research Institute (MSRI) hosted the Clay Mathematics Institute Summer School on the Global Theory of Minimal Surfaces. The nature of the meeting made it possible to give a panoramic view of this subject. The subjects covered include minimal and constant-mean-curvature submanifolds, geometric measure theory and the double-bubble conjecture, Lagrangian geometry, numerical simulation of geometric phenomena, applications of mean curvature

Received by the editors February 12, 2006 and, in revised form, December 20, 2006.
2000 *Mathematics Subject Classification.* 65N22, 35J25, 35B30, 35B65, 49M25, 35D10.
This work was partially supported by the National Science Foundation under the grant NSF-DMS-0305110, and by the Research Fund of Indiana University.

to general relativity and Riemannian geometry, the isoperimetric problem, the geometry of fully nonlinear elliptic equations and applications to the topology of three-dimensional manifolds. An edited book was published in 2005 [10].

The introduction of computer graphics enabled many numerical studies (see for instance [15]). Some of these studies made possible the proof of theoretical results such as the one of Hoffman and Meeks [11].

The problem of non-parametric minimal surfaces consists in finding a graph function u solution of the following minimization functional :

$$\min_{u|_\Gamma=\Phi} \int_\Omega \sqrt{1+|\nabla u|^2}\, dx, \tag{1}$$

for u defined inside Ω, Γ being the boundary of Ω on which Φ is a given L^∞ (or smoother) function.

We recall here that the Euler-Lagrange equation corresponding to (1) and the associated boundary condition read as follows :

$$\operatorname{div}\Big(\frac{\nabla u}{\sqrt{1+|\nabla u|^2}}\Big) = 0, \quad \text{in } \Omega, \tag{2}$$

$$u = \Phi, \quad \text{on } \Gamma. \tag{3}$$

Many works were concerned with the existence of a strong solution for (1) in the case of boundary of non-negative curvature, such as [5], and many others. Since the 1970s, several papers proved the existence of weak solutions of (1) called "generalized solutions" satisfying either $u|_{\Gamma'} = \Phi$ or $\partial u/\partial n(\Gamma') = \infty$, for $\Gamma' \subset \Gamma$: see e.g. [3] and [20] and see also [12] for relevant a priori estimates in a more general context. So the generalized solution develops a "vertical branch" and its normal derivative becomes infinite near the boundary in the region where $u = \Phi$ is not satisfied. Of course here the minimal surface is non-parametric. These results were obtained by two different arguments. On the one hand, Bombieri, De Giorgi and Miranda [3] and Giusti [8] obtained a generalized solution by a purely geometric argument. On the other hand, Temam used in [20] a duality argument and defined also a generalized solution as the limit of sequences of some regularized solutions in the following manner :

$$\min_{u^\varepsilon|_\Gamma=\Phi} \int_\Omega \Big(\frac{\varepsilon}{2}|\nabla u^\varepsilon|^2 + \sqrt{1+|\nabla u^\varepsilon|^2}\Big) dx, \tag{4}$$

i.e.,

$$-\varepsilon\Delta u^\varepsilon - \operatorname{div}\Big(\frac{\nabla u^\varepsilon}{\sqrt{1+|\nabla u^\varepsilon|^2}}\Big) = 0, \quad \text{in } \Omega, \tag{5}$$

$$u^\varepsilon = \Phi, \quad \text{on } \Gamma. \tag{6}$$

Here ε is a small non-negative parameter which may tend to zero. The term $-\varepsilon\Delta u^\varepsilon$ in (5) constitutes an elliptic regularization making the functional in (4) strictly convex and the corresponding Euler equation (5) uniformly elliptic. So, we have by classical theorems the existence and uniqueness of a regular solution ($\mathcal{C}^2(\overline{\omega})$ $\forall\ \omega \subset\subset \Omega$ [1]). It is obvious that this fails to be true up to the boundary

[1] $\omega \subset\subset \Omega$ means $\omega \subset \overline{\omega} \subset \Omega$ as Ω is a bounded open set.

since our data Φ is only $L^\infty(\Omega)$.

We note that the regularized problem has no physical meaning. But it defines a sequence of solutions converging locally, when $\varepsilon \to 0$, to the generalized minimal surface solution as proved in [20]. As a consequence, the regularized solution develops a "boundary layer" near the parts of the boundary where the generalized solution u does not satisfy the boundary condition. In this article, we call "boundary layer" the part of the domain in which the gradient of the solution is very large at least in one direction and depends on a positive and small parameter ε.

1.2. Motivation. In the present article, we mainly study a minimal surface based on a domain Ω which is the interior of an astroid (see Figure (1.a)). Indeed, it is the simplest domain for which the whole boundary has negative curvature. The boundary where the product $x\,y$ is positive (respectively negative) is denoted Γ_1 (respectively Γ_2). See Figure (1.a). Hereafter we assume $\Phi = K1_{\Gamma_1} - K1_{\Gamma_2} \in L^\infty$. Thus, the regularized minimal surface equation and the boundary conditions are given by :

$$\min_{\substack{u|_{\Gamma_1} = +K \\ u|_{\Gamma_2} = -K}} \int_\Omega \Big(\frac{\varepsilon}{2}|\nabla u|^{\,2} + \sqrt{1+|\nabla u|^{\,2}}\Big)dx, \tag{7}$$

and the Euler-Lagrange equation is

$$-\varepsilon\Delta u^\varepsilon - \operatorname{div}\Big(\frac{\nabla\, u^\varepsilon}{\sqrt{1+|\nabla\, u^\varepsilon|^2}}\Big) \;=\; 0, \quad \text{in } \Omega, \tag{8}$$

$$u^\varepsilon = K \quad \text{on } \Gamma_1, \qquad u^\varepsilon \;=\; -K, \quad \text{on } \Gamma_2. \tag{9}$$

Formally, by taking $\varepsilon = 0$ in (7), we obtain again the corresponding nonparametric minimal surface problem which reads :

$$\min_{\substack{u|_{\Gamma_1} = +K \\ u|_{\Gamma_2} = -K}} \int_\Omega \sqrt{1+|\nabla u|^2}\,dx. \tag{10}$$

We note that we have the existence of a generalized solution for (10) thanks to [20]. A solution may be seen in Figure (1b). It looks like a saddle. We call "strong solution" a solution minimizing the functional in (10) and satisfying the boundary condition.

It is interesting to find where the generalized solution detaches from the desired boundary condition and how the domain's geometry plays a fundamental role in this issue. For this purpose, Serrin [16] proved that if the domain's boundary Γ is not of non-negative mean curvature, the generalized solution may be non-regular ($u \neq \Phi$ at the boundary) even if Φ is $\mathcal{C}^\infty$. As the edge of the domain $\partial\Omega$ is not of non-negative mean curvature, we should not expect the existence of strong solution for *any* boundary condition K. We suspect therefore that beyond a critical value K_0, the surface is non-regular. Non-regular means here that either the normal derivative of the generalized solution close to the boundary is infinite or the boundary

condition is not satisfied. The two are equivalent.

In this article, we try to exhibit this regularity loss for the minimal surface solution on the astroid since the mean curvature of its boundary is negative almost everywhere. Such behavior may be studied numerically at any point of the boundary but it is easier to work at points of symmetry such as a corner or the intersection of $\partial\Omega$ and the line $x = y$, namely $I(\sqrt{2}, \sqrt{2})$ (see Figure (1)). In view of the discontinuity of the boundary conditions at the corners, the behavior close to these points is not studied. As a result, we are going to numerically search whether the solution is regular or not at I and find the value of the threshold K_0 above which no strong solution for (10) may exist. Moreover we will provide a generic process to characterize the regularity loss. Another aim of this work is to numerically give a size estimate of this boundary layer versus ε.

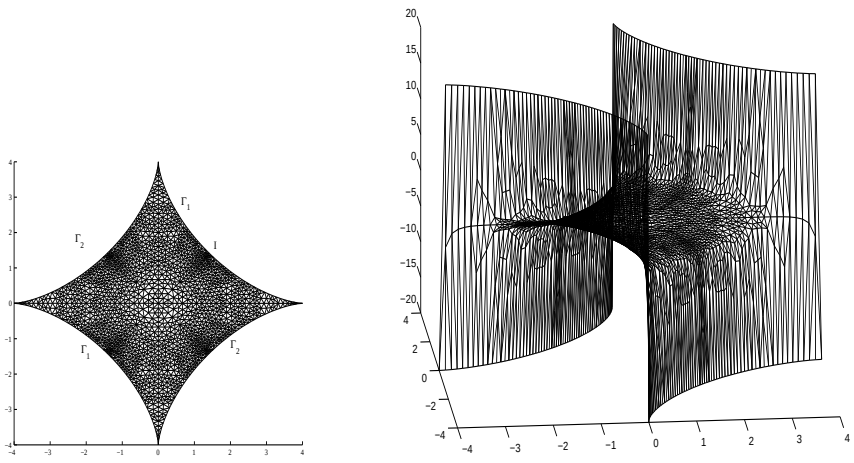

FIGURE 1. The meshed astroid and a typical solution saddle-like ($K = 20$)

After the introduction, the numerical study is given in Section 2. In this Section, we start by presenting our method and validating it. Then, we describe the approaches that were followed even though most of them were not conclusive. We also provide some numerical and theoretical insights into the behavior of the regularized solution when $\varepsilon \to 0$ (the boundary layer behavior). In Section 3, we apply the preceding method to the study of the catenoid, and we conclude in Section 4.

2. Numerical approach

The goal of this study is to determine whether there exists a non-regular solution to the problem (10) and, should it be the case, to find a numerical estimate of K_0 such that for $K \geq K_0$ the generalized solution does not satisfy the boundary conditions. We expect a non-regular solution of (10) and a boundary layer for the regularized problem (4) when ε is small.

Four possible ideas can be employed for a numerical characterization of K_0 :

- for any $K \geq K_0$, the extrapolated value of the solution u_K inside the domain to the point $I(\sqrt{2}, \sqrt{2})$ is K_0 ;
- for any $K, K' \geq K_0$, the difference between u_K and $u_{K'}$ vanishes inside Ω ;

- the slope of the solution gets infinite for $K \geq K_0$;
- for $K \geq K_0$, the numerical resolution does not converge when the mesh gets finer and finer as the solution is no more regular than L^2.

Notice that the two first ideas rely on the characterization of non-regularity by $u|_\Gamma \neq \Phi$ and the two last on $\partial u/\partial n|_\Gamma = \infty$. We explain the numerical method hereafter.

2.1. Numerical method. The numerical method involves three classical steps : constructing the mesh, evaluating the cost function and the (equality) constraints and, mainly, optimizing.

2.1.1. The mesh. The meshes were generated by `emc2` [7] which is included in MODULEF [2]. To speed up the evaluation of the cost function, we meshed only one fourth of the domain, relying on the symmetry for the other quadrangles. We used a spline representation of the astroid's boundary divided into 160 pieces. This spline representation enables angles at the corner of 7E-3 radian. Then `emc2` propagates the mesh inside the astroid.

The angle of the node that coincides with the corner is 0.1 radian for mesh 1 (see Figure (2)), 0.07 radian for mesh 2 and 0.05 radian for mesh 3. As we are interested in the point $I(\sqrt{2}, \sqrt{2})$, and not in the corner, we can assume (this will be partially tested below) that the discretization close to the corner will not product inaccuracies.

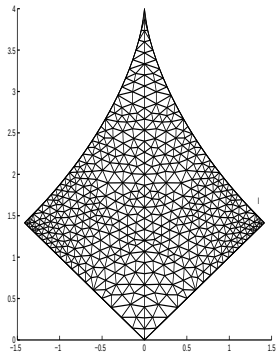

FIGURE 2. One fourth of the domain (mesh 1)

We refined the border close to the point I exponentially. The main data of the meshes are summarized in Table 1.

mesh	summits (`nbs`)	triangles (`nbt`)	number of points on $\Omega \bigcap (x = y)$	ratio of refinement along $x = y$	Δx close to I
1	541	980	20	1.09	3.9E-2
2	2391	4560	50	1.04	1.3E-2
3	4243	8184	80	1.03	6.2E-3

TABLE 1. Main data of the meshes

2.1.2. Numerical evaluation of the functional and constraints. We used a P_1 finite element discretization to compute the non-linear cost function. It has been proved that such a discretization does not converge when minimizing a functional under the constraint of convexity *of the function* u [4]. This is not our case. It is then a standard result that such a discretization converges if u is H^1 (and so ∇u is L^2). On the contrary, for a non-classical solution which is of interest in this article (say L^2 and not H^1 nor $W^{1,1}$), the discretization might not converge.

Although the functional is non-linear, it is simple as it depends only on the gradient which is constant in every triangle for P_1 finite elements. In order to compute it exactly and efficiently, we created two more arrays that stored the derivatives of the local basis functions (the size was $3\times nbt$ where nbt is the number of triangles).

The constraints were evaluated thanks to an array of integers associated to every summit on the boundary. Three different choices of boundary conditions could be settled at the corner (either $+K$, 0 or $-K$). We wondered whether the computed solution could depend on this choice.

2.1.3. Numerical optimization. First, we used MATLAB and `fmincon` from the toolbox `optim`. As one computation needed about 4 days on mesh 2, we gave up after the validation step.

Secondly, we used `DONLP2` [17] [18] that is a free code written either in F77, F90 or C. It is available on the internet. It uses a slightly modified version of the Pantoja-Mayne update for the Hessian of the Lagrangian, variable dual scaling and an improved Armijo-type stepsize algorithm. The CPU time was much less (say a factor 30-40) than MATLAB's routine.

2.2. Validation. Various assumptions have to be tested :

- Does the computed solution depend on the prescribed value at the corners $(0, +K, -K)$?
- Does the computed solution depend on the initial guess ?
- Can we consider mesh 2 or mesh 3 as acceptable ?

2.2.1. Dependence on the corner value. We solved (10) on mesh 2 for $K = 3$ and various prescribed values at the corner $(\pm 4, \pm 4)$. The results are in Table 2. All the expected measures of the singularity close to $I(\sqrt{2}, \sqrt{2})$ gave very similar results. One may notice that the slope along $x = y$ close to I, which will interest us later, depends very weakly ($\simeq 1\%$) on the prescribed value at the corner.

prescribed value	extrapolated (cubic)-K	extrapolated (spline)-K	slope close to I
0	6.4E-3	1.3E-2	12.79
K	6.3E-3	1.29E-2	12.65
$-K$	6.5E-3	1.34E-2	12.92

TABLE 2. Dependence on the corner value

Moreover the differences of the computed solutions are small. If U^0 is the solution computed with a zero prescribed value at the corner, U^K with value K and U^{-K} with value $-K$, then $\| U^0 - U^K \|_{L^2(\Omega)} = 1E-3, \| U^0 - U^{-K} \|_{L^2(\Omega)} = 1E-3$, and $\| U^0 \|_{L^2(\Omega)} = 5.5$. Finally, the difference $U^0 - U^K$ is very localized around the corner. For the sequel we use the zero prescribed value as it is more meaningful.

2.2.2. Dependence on the initial guess. Using zero as the initial guess, MATLAB could compute a solution U_{10} for $K = 10$. Strongly, using this just computed U_{10} as an initial guess to find another U'_{10} took as long as computing U_{10}. The normal gradient (slope) close to I is 76.56 for U_{10} while it is 76.58 for U'_{10}. The L^2 difference of the two solutions is $9.E-07$.

For `donlp2`, the code did not even start, as the gradient is sufficiently small in all the directions.

2.2.3. Dependence on the mesh. In order to prove that our best solution is also a good one, we computed the L^2 norm of the difference of a solution on mesh 2 denoted by U^2_{10} and a solution on mesh 3 U^3_{10} for the same $K = 10$ and $\varepsilon = 0$. The difference is $\| U^2_{10} - U^3_{10} \|_{L^2(\Omega)} = 0.06$ and the L^2 norm of U^2_{10} is 20.7.

We may conclude that results on mesh 3 can be considered as good and even results on mesh 2 are reasonable. We have reached convergence.

2.3. Numerical results. Our aim is to find a good numerical characterization of the regularity loss. Theoretical results propose two ideas : either $u|_\Gamma \neq \Phi$ or $\frac{\partial u}{\partial n}|_\Gamma = +\infty$ at I. Testing the first idea is done in two differents ways in Sections 2.3.1 and 2.3.2. Testing the second idea is done in Sections 2.3.3 and 2.3.4.

2.3.1. Extrapolation of u. The first approach is to extrapolate the solution from *inside* the domain to the point I at the border of the astroid. We expect to find an extrapolated value equal to K_0 for any $K \geq K_0$. Yet, either Piecewise Cubic Hermite Interpolation (PCHI) or piecewise cubic spline interpolation (SPLINE) give results so close to the identity function that only their *difference* with K is given in Figure 3 for mesh 2. Even though a kind of rupture can be guessed on Figure 3 at about $K = 3$, the difference of the extrapolated value with K has no obvious link with K_0.

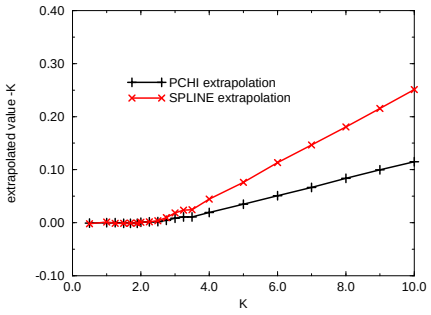

FIGURE 3. Difference of the extrapolated value (two methods) with $K \mapsto K$

Three other tools provided by MATLAB to extrapolate gave infinite values, even for "small" K such as $K = 1$ (at this stage we have no idea of K_0).

One may explain the discrepancy with our expectation by saying that the numerical code provided a too regular solution. It does not seem to catch the (assumed) non-regularity. Here, the non-regularity is a drawback to measure K_0. It will be an advantage further.

2.3.2. Difference of U_K and $U_{K'}$. The second approach is to look at the difference $U_K - U_{K'}$ as a function of K, K'. We expect the difference to vanish inside the domain for K and K' greater than K_0 as, then $\gamma_0(U(K)) = \gamma_0(U(K'))$ and the functional does not depend on K.

It happens that the difference of the *computed* U_K and $U_{K'}$ does not vanish at the boundary (its value is $K - K'$). To overcome this error, we evaluate the difference by removing the triangles which have an edge on the boundary. So we draw a slightly modified version of $|U_{K+1} - U_K|_{L^2}/|U_K|_{L^2}$ on Figure 4. This very crude graph is difficult to interpret as no abrupt change appears. The undrawn figures of $|U_K - U_{40}|_{L^2}/|U_{40}|_{L^2}$ and $|U_K - U_{40}|_{L^2}/|U_{40}|_{L^2}$ provide no more conclusion. This approach is unreliable.

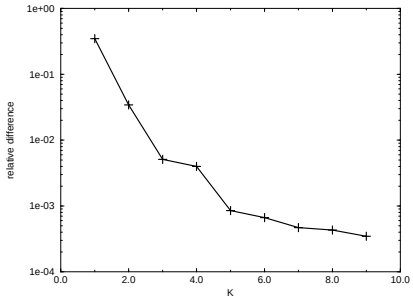

FIGURE 4. Relative difference between U_K and U_{K+1} (L^2 norm)

2.3.3. Infinite slope. None of the preceding means using the values of u provided a result. Although measuring a slope is less accurate (and more sensitive !), we tried the third approach which consists in drawing the normal gradient (or normal slope) close to I for mesh 1, mesh 2 and mesh 3 in Figure 5.

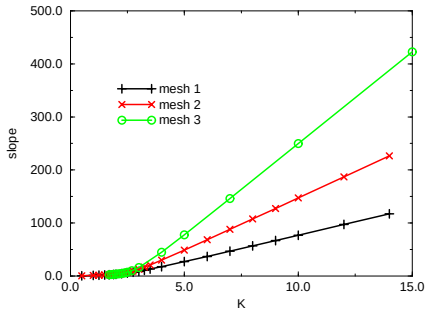

FIGURE 5. Slopes versus K

No discontinuity (as a signal of infinity) could be detected, but Figure 5 led us to use the last mean : once K is greater than K_0, the exact slope is infinite and so the discretized one should be mesh dependent. The non-convergence is no more a drawback : it is useful.

2.3.4. Slope depending on the mesh for $K \geq K_0$. The fourth approach uses the fact that the solution we are interested in is non-regular. So it should not converge as can be partially seen on Figure 5 which gives a rough estimate of the value of K_0 between 2 and 4. Zooming in the range $K \in [0.1, 3]$ shows little discrepancy between the results on the three meshes but the discrepancy increases rather continuously. Obviously for $K > 4$, the more we refine, the greater the slope is. The very clear change between $K < 2.5$ and $K \geq 4$ enables us to guess that there exists a threshold K_0 such that if $K > K_0$ the associated solution to (10) in an astroid is no more regular close to I.

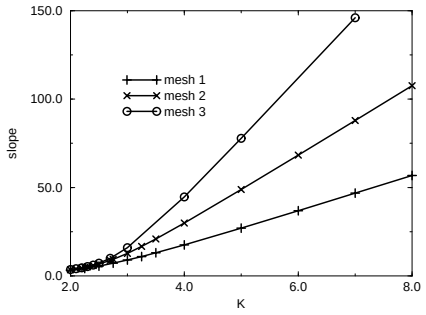

FIGURE 6. More localized computations of the slopes versus K

A zoom leads us to the Figure 6. Yet, the Figure 6 is less precise than making a linear regression from Figure 5 in the straight parts of the curves (almost exactly linear). All these lines meet at the same point whose abscissa is 3 ± 0.2 *which is here the numerically estimated value of* K_0.

We also used a mesh uniformly as fine as mesh 2 close to I ($\Delta x \simeq 1.E-2$). Computations not provided here on this mesh gave a normal slope at I close to that of mesh 2. It proves that only the precision in the vicinity of the point I is crucial. Moreover, the number of evaluations of the cost function and time of computation increases from $K = 3$ but this is not a serious criterion for finding K_0.

One may find about the same value (3 ± 0.2) from the difference of the numerically measured normal slopes between mesh 2 and mesh 3 on Figure 7.

2.4. Dependence of the boundary layer on the regularization. An asymptotic analysis enables us to guess the order of the boundary layer from the equation. First we need some preliminary results.

Introducing a new system of coordinates ; $z = (x+y)/\sqrt{2}$, $t = (x-y)/\sqrt{2}$ and $v(z,t) = u^\varepsilon(x,y)$, we state the following theorem.

THEOREM 1. *The solution $v(z,t)$ of the regularized equation (8)-(9) inside an astroid has a trace along the axis of symmetry $t = 0$ that satisfies for all ε :*

$$\varepsilon\left(\frac{\partial^2 v}{\partial z^2} + \frac{\partial^2 v}{\partial t^2}\right) + \frac{\partial^2 v/\partial z^2}{\left(1 + (\partial v/\partial z)^2\right)^{3/2}} + \frac{\partial^2 v/\partial t^2}{\left(1 + (\partial v/\partial z)^2\right)^{1/2}} = 0. \tag{11}$$

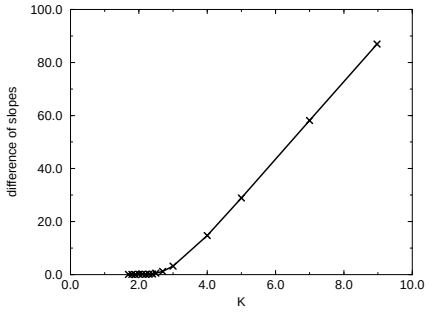

FIGURE 7. Difference of normal slopes between mesh 2 and mesh 3

Moreover, at the point $I(\sqrt{2},\sqrt{2})$*, any such function* $v(z,t)$ *such that* $v|_{\Gamma_1} = +K$ *and* $v|_{\Gamma_2} = -K$ *is odd in* t *and satisfies :*

$$\frac{\partial^2 v}{\partial t^2} = -1/6 \frac{\partial v}{\partial z}. \tag{12}$$

Sketch of the proof

The proof of (11) is straightforward. Concerning the proof of (12), it suffices to make an expansion of the function $v(z,t)$, to use the fact that derivatives of v odd in t are zero along the segment $t = 0$ by symmetry. The symmetry of the geometry proves that the solutions are odd in t.

The solution $v(z,t)$ is constant on Γ_i. An expansion in $\theta - \pi/4$ of the solution leads to (12). By pursuing the expansion, one might even prove that

$$54\frac{\partial^3 v}{\partial z \partial t^2}(2,0) + 9/2\frac{\partial^2 v}{\partial z^2}(2,0) + 54\frac{\partial^4 v}{\partial t^4}(2,0) - 30\frac{\partial^2 v}{\partial t^2}(2,0) - 13/4\frac{\partial v}{\partial z}(2,0) = 0.$$

□

The equation (11) of Theorem 1 also reads :

$$\varepsilon\Big(\frac{\partial^2 v}{\partial z^2} + \frac{\partial^2 v}{\partial t^2}\Big)\left(1 + (\frac{\partial v}{\partial z})^2\right)^{3/2} + \frac{\partial^2 v}{\partial z^2} + \frac{\partial^2 v}{\partial t^2}\Big(1 + (\frac{\partial v}{\partial z})^2\Big) = 0, \quad \text{at } t = 0. \tag{13}$$

Let us assume the boundary layer is of size ε^α. Then if we let $z = \varepsilon^\alpha Z$ and use this in (12), one sees that the second derivative in t close to I will be negligible with respect to $\partial^2 v/\partial z^2$ which is of order $\varepsilon^{-2\alpha}$. We thus recover the well-known result that in a boundary layer the most important variation holds in the normal direction (z direction in our case). But this negligibility is limited as $\partial^2 v/\partial t^2 = -(\varepsilon^{-\alpha}/6)\ \partial v/\partial Z$ and $\partial^2 v/\partial z^2 = \varepsilon^{-2\alpha}\partial^2 v/\partial Z^2$.

Then the leading terms in the equation (13) are given by

$$\varepsilon^{1-5\alpha}\frac{\partial^2 v}{\partial Z^2}\left(\frac{\partial v}{\partial Z}\right)^3 + \varepsilon^{-2\alpha}\frac{\partial^2 v}{\partial Z^2} + \varepsilon^{-2\alpha}\frac{\partial^2 v}{\partial t^2}(\frac{\partial v}{\partial Z})^2 = 0, \quad \text{at } t = 0, \tag{14}$$

sufficiently close to I (to have (12)). One must notice that the equation (12) makes the second term negligible with respect to the third one. Had we neglected

all the t derivatives, we would have been led to a different result. Then by homogeneity we obtain $1 - 5\alpha = -3\alpha$ or $\alpha = 1/2$. Of course here we just intend to get an order of magnitude of the boundary layer and a complete study of this problem is postponed to a subsequent work.

Now, we are going to numerically check the value found by our simple asymptotic analysis. For this purpose, we look for the regularized solution, extract the slope and draw its variation with the regularizing parameter ε in the left part of Figure 8. The computations are done on mesh 3 and K is set equal to 20. The normal slope as a function of ε varies approximatively as $\varepsilon^{-\alpha}$ with $\alpha \simeq 0.4$ for mesh 3 (astroid). This is compatible with what we expected from our asymptotic analysis.

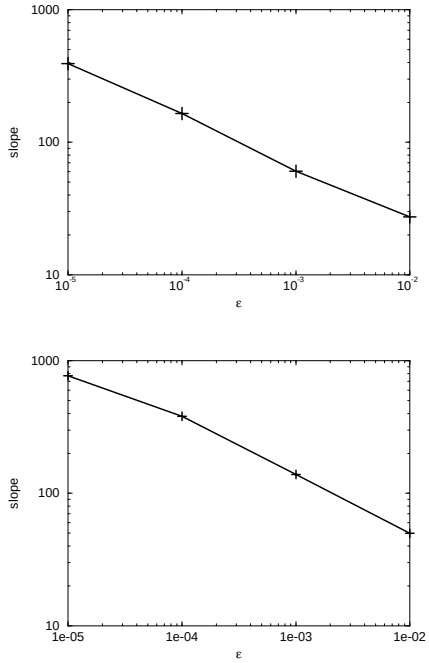

FIGURE 8. Dependence on ε of the normal slope in the astroid (left-mesh 3) and the catenoid (right-mesh 4)

3. The case of the catenoid

In order to check our numerical method, we need a test case where the exact value of the threshold is known exactly. This is the case for the (non-parametric) catenoid where the exact value of K_0 is $K_0 = R_1 \ln\left((R_2 + \sqrt{R_2^2 - R_1^2})/R_1\right)$ (see for instance [9]). For $R_1 = 1, R_2 = 2$, it is about 1.32.

In order to find the catenoid, we mesh non-radially a fourth of an annulus and solve (10) with DONLP2 (cf. [17], [18]). Then we read the normal gradient along a section radially uniformly meshed with 20, 30, 50 or 100 points. The results are reported on Figure 9. When one draws the four straight lines for each mesh after the non-convergence, there is, like in the astroid case, only one intersection. Its

abscissa is $K \simeq 1.28$. This numerical value is sufficiently close to the exact one (about 1.32) to give confidence. *A posteriori*, it gives one more argument for the study in the astroid.

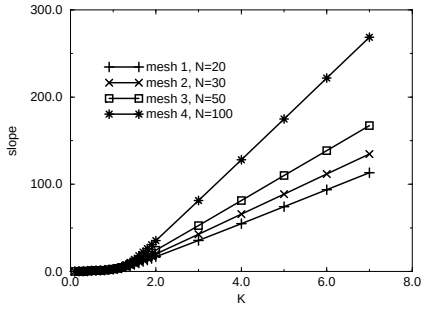

FIGURE 9. Normal gradient on the interior circle (catenoid)

Like in the astroid case, one may draw the difference of the computed slopes as a function of K for the two best meshes. Such a curve is drawn in Figure 10. Like for the astroid, it drives us to predict a value $K \simeq 1.4$ which is reasonable.

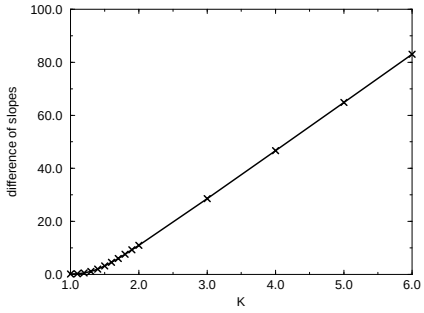

FIGURE 10. Difference of normal gradient on the interior circle (catenoid)

Let us notice that even if the meshes had increasing number of points along one section, the rest of the meshes was not equally refined. The data of these four meshes are summarized in Table 3 in one fourth of the annulus. We also drew in Figure (8b) the slope of the regularized catenoid as a function of the regularizing parameter ε. While the theoretical value of the slope is $1/3$ (see [9]) we found a reasonable value of 0.38.

4. Conclusion

Some conclusions may be drawn from the preceding study. One may be convinced that there exists no regular solution to the problem (10) in an astroid for K above a certain value K_0. An estimate for this threshold in an astroid is $K_0 = 3 \pm 0.2$. The nature of the convergence of the regularized solution to the non-regularized one can be seen on Figure 8.

mesh	summits	triangles	number of points on the radial section
mesh 1	985	1848	20
mesh 2	2161	4140	30
mesh 3	2482	4762	50
mesh 4	1650	3132	100

TABLE 3. Main data of the meshes of the catenoid

All these computations are checked in the case of the catenoid for which the exact threshold K_0 is known, see [9].

Last but not the least, "natural" approaches could be very deficient. Using the numerical non-convergence as a sign of non-regularity is more powerful than any extrapolation. This is confirmed by the study on the catenoid and should be taken into account in future computations on these generalized solutions to the minimal surface problem. Even outside the field of optimization, any numerical attempt to characterize the regularity loss could use the numerical process given in this article.

Acknowledgments

We are grateful to Professor Roger Temam for introducing us to the subject and for his helpful suggestions during all the work.

References

[1] F.J. Almgren *Existence and regularity almost everywhere of solutions to elliptic variational problems with constraint,* Mem. A.M.S. 4 n.165 1976.
[2] M. Bernadou, *et al. MODULEF: une bibliothèque modulaire d'éléments finis.* (French) [MODULEF: a modular library of finite elements] Second edition. Institut National de Recherche en Informatique et en Automatique (INRIA), Rocquencourt, 1988.
[3] E. Bombieri, E. De Giorgi and M. Miranda, *Una maggiorazione a priori relativa alle ipersuperfici minimali non parametriche.* (Italian) Arch. Rational Mech. Anal. **32** (1969) 255–267.
[4] P. Choné and H.V.J. Le Meur, *Non-convergence result for conformal approximation of variational problems subject to a convexity constraint.* Numer. Funct. Anal. Optim. 22 (2001), no. 5-6, 529–547.
[5] J. Douglas, *Solution of the Problem of Plateau.* Trans. Amer. Math. Soc. 33, 263-321, 1931.
[6] L. Euler *Methodus inveniendi lineas curvas maximi minimive proprietate gaudentes sive solutio problematis isoperimetrici latissimo sensu accepti*, Lausanne and Geneva 1744 = OPERA, I, Vol. XXIV, C. Carathéodory, Ed. Bern, 1952.
[7] P.L. Georges http://www-rocq.inria.fr/modulef/Doc/GB/Guide3-14/welcome.html.
[8] E. Giusti, *Minimal surfaces and functions of bounded variation.* Monographs in Mathematics, 80. Birkhäuser Verlag, Basel, 1984.
[9] M. Hamouda, *Asymptotic analysis for the regularized minimal surface problem in the radially symmetric case,* Asymptotic Analysis **32** (2002), no. 2, 107–130.
[10] D. Hoffman, Editor, *Global theory of minimal surfaces.* Proceedings of the Clay Mathematical Institute Summer School held in Berkeley, CA, June 25–July 27, 2001. Edited by David Hoffman. Clay Mathematics Proceedings, 2. American Mathematical Society, Providence, RI; Clay Mathematics Institute, Cambridge, MA, 2005.
[11] D.A. Hoffman and W. Meeks III, *A complete embedded minimal surface in R^3 with genus one and three ends.* J. Differential Geom. 21 (1985), no. 1, 109–127.
[12] O. A. Ladyzenskaya and N. N. Uralceva, Local estimates for gradients of solutions of non-uniformly elliptic and parabolic equations. Comm. Pure Appl. Math. **18**, 677-703 1970.
[13] J.L. Lagrange, *Oeuvres* Lagrange à Euler. Die 12 augusti [1755], Vol. XIV pp. 138-144.
[14] J.A.F. Plateau *Statistique expérimentale et théorique des liquides soumis aux seules forces moléculaires*, Gauthiers-Villard, Paris 1873.

[15] H. Rosenberg and D. Hoffman, *Surfaces minimales et solutions de problèmes variationnels [minimal surfaces and solutions of variational problems]* SMF Journée Annuelle [SMF annual Conference], 1993. Société Mathématique de France, Paris 1993.
[16] J. Serrin, *The problem of Dirichlet for quasilinear elliptic differential equations with many independent variables,* Philos. Trans. Roy. Soc. London, Ser. A **264** (1969), 413-496.
[17] P. Spellucci, *An SQP method for general nonlinear programs using only equality constrained subproblems.* Math. Programming 82 (1998), no. 3, Ser. A, 413–448
[18] P. Spellucci, *A new technique for inconsistent QP problems in the SQP method.* Math. Meth. of Oper. Res. 47 (1998) 355-400 (Physica Verlag Heidelberg, Germany
[19] J.E. Taylor *Singularities in minimal surfaces* Ann. Math. 103 (1976), 489-539.
[20] R. Temam, *Solutions généralisées de certaines équations du type hypersurfaces minima.* (French) Arch. Rational Mech. Anal. 44 (1971/72), 121–156.

University of Carthage 7 November. Faculty of Sciences of Bizerte. Jarzouna 7021, Tunisia.
E-mail: Makram.Hamouda@math.u-psud.fr
URL: http://www.math.u-psud.fr/∼hamouda/

CNRS, Laboratoire de Mathématiques d'Orsay, Orsay cedex, F-91405; Univ Paris-Sud, Orsay cedex, F-91405.
E-mail: Herve.LeMeur@math.u-psud.fr
URL: http://www.math.u-psud.fr/∼lemeur/